Second-harmonic generation

(how to get from a wavelength of 980 to 490 nm)

Michiel .J.A. de Dood
Huygens Laboratorium 909a, tel. 071-527 5929

January 24, 2006

Abstract

The goal of this experiment in nonlinear optics is to study the conversion of a (very small) fraction of laser light from its original wavelength of 980 nm (i.e. invisible to the naked eye) to its second-harmonic at a wavelength of 490 nm. This conversion takes place by mild focussing of an intense laser beam in a nonlinear birefringent crystal of BBO (= β $BaBO_4$). You will study the physical processes that determine the nonlinear conversion and hopefully appreciate the central role of phase matching. These phase matching conditions ensure that the generated second harmonic light interferes constructively in the forward propagating direction. Angle tuning of the birefringent crystal allows you to change the phase matching conditions through changing the refractive indices. Playing with the geometry, the various polarizations, angles, and crystals you will hopefully be rewarded with a very weak blue beam at the nanoWatt level, starting with a dangerously strong infrared beam of tens of milliWatts. Please be careful, read the required safety procedures carefully, and follow them strictly; we don't want you to hurt yourself or somebody else!

1 Introduction

Under normal conditions the response of a medium to light is linear and as a consequence most optical phenomena can be described with a linear refractive index. It was only with the invention of lasers in the early 1960's that the available optical power level increased to a level where the response of the medium started to deviate from the linear behavior. It was found that at sufficiently high light intensities the response of the material depends on the light intensity. This led to an entirely new field of nonlinear optics and the discovery of various intriguing phenomena such as second harmonic and sum- and difference frequency generation [1, 2].

Nowadays, frequency conversion is a common tool to create blue or infrared laser light in the laboratory; i.e. at frequencies where no alternative laser sources are available. This experiment will explore the process of second harmonic generation by

studying the conversion of a high power infrared beam at a wavelength of 980 nm into blue light at a wavelength of 490 nm.

2 Theory

2.1 Non-linear Optics

The optical response of a material is expressed in terms of the induced polarization $\vec{P}$. For a linear material the relation between the polarization and the electric field $\vec{E}$ of the incident radiation is linear:

$$\vec{P} = \varepsilon_0 \chi^{(1)} \vec{E}, \tag{1}$$

where $\chi^{(1)}$ is the well-known linear susceptibility ($n^2 = \varepsilon_r = 1 + \chi^{(1)}$).

In nonlinear optics, the response of the material is often be described as a Taylor expansion of the material polarization $\vec{P}$ in powers of the electric field $\vec{E}$. Using the Einstein summation convention, each component P_k ($k = x, y, z$) of the material polarization can be expressed as:

$$P_k = \varepsilon_0 \left(\chi^{(1)}_{ik} E_i + \chi^{(2)}_{ijk} E_i E_j + \chi^{(3)}_{ijlk} E_i E_j E_l + \ldots \right) \tag{2}$$

Here, the coefficients $\chi^{(n)}$ correspond to the tensor of the n-th order nonlinear process. For most practical applications that consider a specific non-linear process in a well defined direction, the tensor can be reduced to a single effective nonlinear coefficient. Let us consider only the second order term and calculate the resulting nonlinear polarization, i.e. $P_k(NL) = \chi^{(2)}_{ijk} E_i E_j$ for a harmonic field input field at frequency ω. The harmonic input field is given by:

$$E_i = \mathcal{E}_i \exp(-i\omega t) + c.c., \tag{3}$$

where $\mathcal{E}_i$ is the field amplitude at a given position. The resulting second order non-linear polarization is easily found to be:

$$P_k(NL) = \chi^{(2)}_{ijk} \left(\mathcal{E}_i \mathcal{E}_j \exp(-i2\omega t) + \mathcal{E}^*_i \mathcal{E}^*_j \exp(i2\omega t) + \mathcal{E}_i \mathcal{E}^*_j + \mathcal{E}^*_i \mathcal{E}_j \right) \tag{4}$$

From the above expression it is immediately clear that the non-linear polarization contains a component that radiates at twice the frequency of the input light. The second order polarization also contains a component at frequency zero, an effect known as optical rectification. In the remaining we will ignore this DC electrical field and discuss only the second harmonic.

An important symmetry aspect of the above Taylor expansion is that all even-order coefficients must disappear for media with inversion symmetry. The explanation is simple: the operation $\vec{r} \rightarrow -\vec{r}$ leaves the inversion-symmetric media unaffected, but does add minus signs to both $\vec{P} \rightarrow -\vec{P}$ and $\vec{E} \rightarrow -\vec{E}$. This is only possible when $\chi^{(n)} = 0$ for even n. Note that most materials do have inversion symmetry and second harmonic generation can therefore only be observed in a very specific class of non-linear crystals.

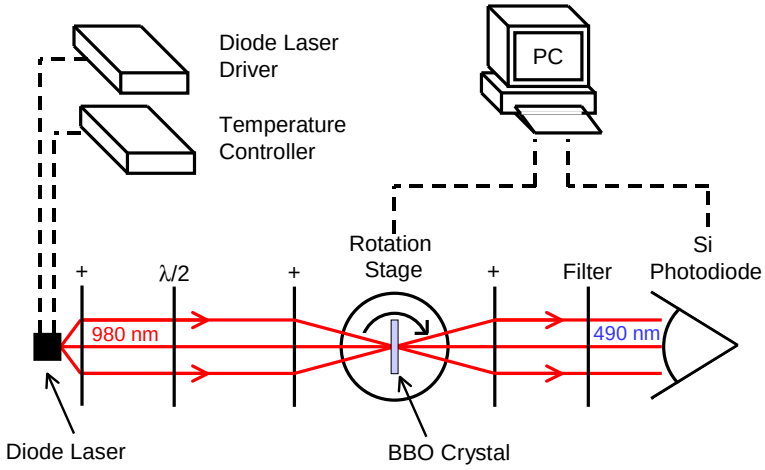

Figure 1: *Experimental setup used for the second-harmonic generation. An incident beam from a diode laser at a wavelength of 980 nm is focused into a crystal of BBO. Here a small fraction of the incident light is converted into light at the double frequency leading to a faint blue beam at a wavelength of 490 nm. The 490 nm light is filtered out and its intensity can be measured using a sensitive photodiode.*

Even if this inversion symmetry is broken, the resulting second-order non-linearity is extremely weak. As a rule of thumb the relative weight of the nonlinear terms is determined by the strength of the incident electro-magnetic field as compared to the atomic field, i.e. $\chi^{(n)}/\chi^{(1)} \propto (E/E_{atom})^{n-1}$. For weak to moderate incident fields the material response is linear to a very good approximation. At larger fields higher-order terms in the Taylor expansion become noticeable as the response of the charged particles inside the atoms becomes nonlinear. At extremely large fields ($E \geq E_{atom}$) the Taylor expansion breaks down and the electrons are ripped from the atoms via optical field ionization. For comparison: In the present experiment we focus a laser beam of 50 mW (being about 50x more intense than a typical HeNe laser used in previous experiments) down to spot diameters of a few tens of μm, to produce intensities of $I \leq 10^8$ W/m^2. Although dangerously strong, the associated electric fields are still very small as compared to atomic fields, which are typically 1 V per Angstrom or $E = 10^{10}$ V/m, corresponding to optical intensities of $I \approx 10^{17}$ W/m^2.

Because of the relative strength of the non-linear coefficients it is logical that the first nonlinear optical process to be discovered was second-harmonic generation, in which a small fraction of the incident laser light is converted into light at twice the incident frequency. You will study this process with the setup depicted in Fig. 1, where the actual conversion takes place by focusing a laser beam in a crystal of β $BaBO_4$ (in short BBO). This material is optically transparent in the visible, has no inversion-symmetry and has a relatively large $\chi^{(2)}$ coefficient. Still, a relative powerful infrared (980 nm) semiconductor laser is needed to create a very weak blue (490 nm) beam.

For completeness we note that the conversion efficiency can be greatly enhanced

by (i) resonant excitation inside an optical cavity, which increases the average optical intensity, or (ii) pulsed instead of continuous wave (cw) excitation, which increases the peak intensity. None of these techniques will be tried here.

2.2 Second-harmonic generation as two-step process

Comprehensive theories of second-harmonic generation have been developed in the late sixties by among others Boyd [3, 4]. We will present a modest summary below (see also [1]), which should contain enough information for the present experiment. The basic idea of most theories in nonlinear optics is that the incident optical field is generally very small compared to the atomic fields, so that nonlinear effects can be treated as weak perturbations on top of the ordinary linear optics. Our theoretical discussion of second-harmonic generation thus proceeds in two steps. In the first step the incident field E_1 at frequency ω excites a weak nonlinear polarization at the double frequency $P_2 \propto E_1^2$. In the second step this induced nonlinear polarization P_2 radiates according to Maxwell's equations and emits an optical field E_2 at optical frequency 2ω.

The second harmonic light originates from the non-linear polarization. The input wave generates a set of dipoles inside the crystal that all radiate weakly at twice the frequency of the input wave. As the input beam has a well defined phase and amplitude at every point inside the crystal at a given time, the relative phase of the induced dipoles is fixed. To obtain a second harmonic output at the end of the crystal it is important that the induced dipoles radiate in phase, as depicted in Fig. 2. This process is referred to as phase-matching which ensures that the contributions from all positions in the crystal add up constructively. We will first introduce the concept of phase-matching using plane waves. We will then discuss how this can be achieved in practice using birefringent materials and finally introduce a more formal theory and show how focussed beams can be used to boost the efficiency of the process.

2.3 Second-harmonic generation for "plane waves"

For plane waves, the generation of second harmonic radiation becomes relatively simple. This plane-wave limit is reached in practice when a laser beam is wide enough to neglect the effect of focusing. In this case, the spatial part of the incoming wave in Fig. 2 is proportional to $\exp(i\vec{k_\omega}\vec{r})$, where k_ω is the wave vector of the incident light at frequency ω. Let us assume for simplicity that we look at a collinear process where the fundamental and second harmonic beam propagate in the positive z direction, so that $\vec{k_\omega} = k_{z,\omega}$. The non-linear crystal has a thickness L and extends from $z = 0$ to $z = L$.

At every position in the crystal, the non-linear polarization creates a dipole emitter that radiates at twice the fundamental frequency. At every time the relative phase of these dipoles is given by the non-linear polarization generated by the fundamental wave: $\exp(ik_{z,\omega}z)^2 = \exp(i2k_{z,\omega}z)$. The plane waves emitted in the forward direction are plane-waves at double the frequency and have the form $\exp(-ik_{z,2\omega}z)$. The overall efficiency of this process in the forward direction is obtained by adding all contributions

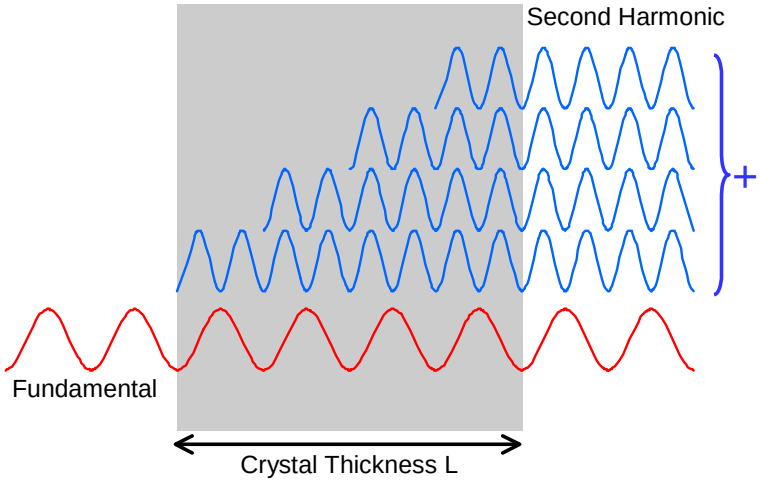

Figure 2: *A sketch of the concept of phase matching. The fundamental wave at frequency ω has a well defined phase and amplitude everywhere in the crystal. The induced dipoles all radiate at a frequency 2ω with a phase dictated by the fundamental wave. The picture shows the case where all dipoles radiate in phase in the forward direction so that all contributions add up constructively.*

from different positions. This leads to the following integral that gives the conversion efficiency per unit length (in terms of intensity) of the process:

$$\eta = \frac{1}{L^2}\left|\int_0^L \mathrm{e}^{(i2k_\omega z)}\mathrm{e}^{(-ik_{2\omega}z)}\mathrm{d}z\right|^2 = \frac{1}{L^2}\left|\int_0^L \mathrm{e}^{(i\Delta kz)}\mathrm{d}z\right|^2 = \left(\frac{\sin(\Delta kL/2)}{\Delta kL/2}\right)^2, \quad (5)$$

where $\Delta k = 2k_\omega - k_{2\omega}$ is the wavevector mismatch of the process. This sinc function has a maximum for $\Delta k = 0$ where $\eta = 1$.

It is important to realize at this point that ordinary materials display natural frequency dispersion (= frequency dependence of the refractive index). Most materials that are transparent in the visible, have a refractive index that decreases with increasing wavelength. The corresponding wavevector mismatch $\Delta k = 2\omega n(\omega)/c - 2\omega n(2\omega)/c < 0$. It is therefore impossible to achieve efficient second harmonic generation in these materials, unless a way is found to phase-match the interaction. As we will see, birefringent materials offer a way to achieve $\Delta k = 0$. Angle-tuning of these birefringent crystals is *the technique* to modify the refractive indices and tune the phase matching.

2.4 Birefringence

In birefringent (or double-refracting) crystals the refractive index depends not only on wavelength, but also on the polarization direction of the light relative to the crystal

axes. In essence, by choosing the polarization of the second harmonic and the input beam to be orthogonal one can use this birefringence to compensate for the natural index dispersion and achieve perfect phase-matching.

Here we will consider uniaxial crystal that have one axis (the so-called c-axis) that is different from the two other identical axis. To describe the propagation of light inside such a crystal, the electric field vector of the light wave is decomposed in a component parallel to the c-axis and a component perpendicular to the c-axis. Electric field components perpendicular to the c-axis propagate according to the *ordinary refractive index* $n_o(\lambda)$, whereas the orthogonal field components propagate according to the so-called *extra-ordinary index* $n_e(\theta, \lambda)$. The refractive index seen by these extra-ordinary rays depends on the angle θ between the rays and the crystalline c-axis, via:

$$\frac{1}{n_e(\Theta,\lambda)^2} = \frac{\sin\Theta^2}{n_e(\lambda)^2} + \frac{\cos\Theta^2}{n_o(\lambda)^2}, \tag{6}$$

with as limiting case $n_e(0^\circ, \lambda) = n_0(\lambda)$ (no difference for propagation along c-axis) and $n_e(90^\circ, \lambda) = n_e(\lambda)$ (maximum difference for propagation perpendicular to c-axis). This relation is depicted graphically in Fig. 3. A line starting at the origin intersects the two curves and gives the ordinary and extra-ordinary refractive index for a particular choice of the angle θ with the c-axis. The solid circle corresponds to the ordinary refractive index that is independent of the angle θ. The dashed line describes an ellipsoid that corresponds to the extra-ordinary index.

The BBO crystals used in the experiment are birefringent and obey the above relation for $n_e(\Theta, \lambda)$; their wavelength-dependent refractive indices $n_o(\lambda)$ and $n_e(\lambda)$ are depicted in Fig. 4 (data taken from http://www.eksma.lt).[1] As the extra-ordinary index is smaller than the ordinary one (one speaks about *negative* birefringent crystals) the phase-matching condition can only be reached if the polarization direction of the primary light is ordinary, while the second-harmonic light has an extra-ordinary polarization. Phase matching for the conversion 980 nm $\rightarrow$ 490 nm is then reached for rays at an angle of 24.9° with the c-axis, where $n_o(980\ nm) = 1.657$, $n_e(490\ nm) = 1.560$ and $n_o(490\ nm) = 1.681$, making $n_e(24.9^\circ, 490\ nm) = 1.657$ (indicated by the horizontal line in Fig. 4).

The crystals used in the experiment are cut in such a way that the so-called cut angle Θ_c, being the angle between the crystalline c-axis and the surface normal is very close to phase matching for ordinary-polarized 980 nm light and extra-ordinary-polarized 490 nm light, i.e. $\Theta_c \approx 24.9^\circ$. As phase matching is quite critical in second-harmonic generation, the effect of small angle tuning on the extra-ordinary refractive index can easily be calculated from a Taylor expansion of the angle-dependence of $n_e(\Theta, \lambda)$. The crucial derivative here is the so-called transverse walk-off angle ρ via

$$\tan\rho \equiv \frac{1}{n_e(\Theta)}\left|\frac{\partial n_e(\Theta)}{\partial\Theta}\right| \approx \left|\frac{\partial n_e(\Theta)}{\partial\theta}\right|, \tag{7}$$

[1] The refractive indices of BBO are given by the following equations: $n_o(\lambda)^2 = 2.7405 + 0.0184/(\lambda^2 - 0.0179) - 0.0155\lambda^2$,$n_e(\lambda)^2 = 2.3730 + 0.0128/(\lambda^2 - 0.0156) - 0.0044\lambda^2$, with λ being the wavelength in microns ($0.3 < \lambda < 2.0$)

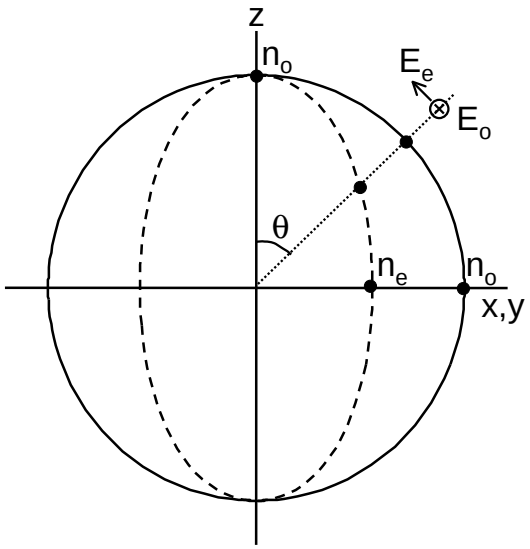

Figure 3: *Plot (exaggerated!) of the ordinary and extra-ordinary refractive index at a single wavelength for different propagation directions. A line from the origin corresponds to propagation at an angle θ relative to the c-axis. The two intersections yield the ordinary and extra-ordinary refractive index. The direction of the E-field for ordinary and extra-ordinary polarization is sketched in the figure as well.*

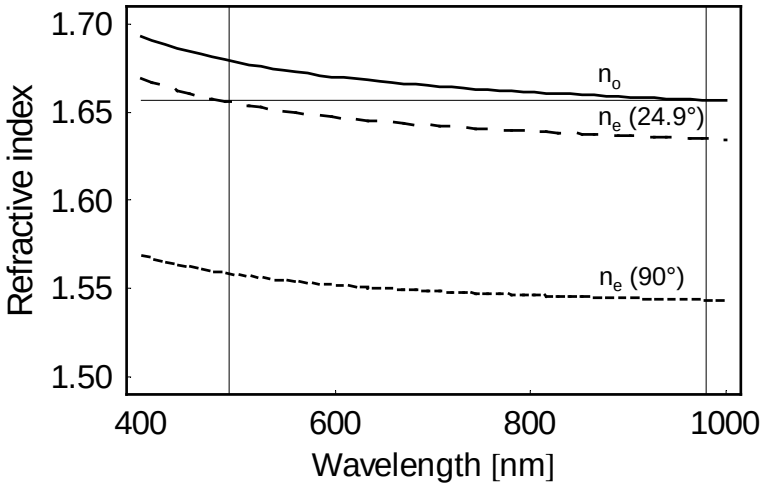

Figure 4: *Refractive index as a function of optical wavelength for BBO. The lines in the figure correspond to the ordinary and extra-ordinary refractive index. Also indicated is the index calculated for $\theta = 24.9^\circ$ that yields perfect phase matching for frequency doubling of 980 nm light.*

where the pre-factor $1/n_e(\Theta)$ takes cares of the conversion from external tuning angles θ to internal angles Θ, via Snell's law $\sin\theta = n_e(\Theta)\sin\Delta\Theta$.

The transverse walk-off angle ρ also appears in a different and even more important context. The propagation of light with extra-ordinary polarization is truly extra-ordinary in the sense that the direction of energy flow, given by the Pointing vector $\vec{S} \propto \vec{E} \times \vec{H}$, can differ from the direction of the optical momentum $\vec{k} \propto \vec{D} \times \vec{H}$, just because the relative dielectric constant is a tensor instead of a scalar. Looking through a birefringent crystal one generally observes two shifted images, one for each polarization, as demonstrated in many textbooks. The angle between $\vec{S}$ and $\vec{k}$ is called the transverse walk-off angle ρ. It will show up in several places in the discussion below, where it quantifies the walk-off angle between the extra-ordinary polarized 2ω light and the fundamental ω light. For BBO crystal at $\Theta_c = 24.9$ and $\lambda = 490$ nm the walk-off angle can be calculated to be $\rho = 60$ mrad.

The wavevector mismatch $\Delta k \equiv 2k_\omega - k_{2\omega}$ plays an essential role int process of second-harmonic generation and can be varied experimentally by angle tuning. A Taylor expansion of the phase mismatch $\Delta kL/2$ in the tuning angle θ between crystal and incident beam yields

$$\tfrac{1}{2}\Delta kL = \frac{2\pi}{\lambda}\left(2n_e(\Theta,\lambda/2) - 2n_o(\lambda/2)\right)\frac{L}{2} \approx \frac{2\pi L|\rho|}{\lambda}\theta, \tag{8}$$

where λ is the wavelength of the fundamental input wave. The absolute sensitivity of second-harmonic generation to angle tuning is most easily expressed via the crystal angle tolerance T, which is just a rewrite of the walk-off angle ρ and specifies the angular width of the resonance curve. For our BBO crystal and conversion geometry T = 4.8 mrad.mm, which corresponds to an angular width of 4.8 mrad for a 1 mm thick crystal and 2.4 mrad for a 2 mm crystal.

2.5 Second-harmonic generation of focussed beams

The generated intensity of second harmonic light scales quadratically with the input intensity. By focussing the light to a tiny spot it is possible to gain enormously. Observing the frequency doubled light with true plane waves is next to impossible, while you should be able to see the blue light by eye when you use a strongly focussed beam. Although the principle of phase-matching derived for plane-waves remains a valid concept, it is necessary to summarize a more formal theory to understand second harmonic generation when the input and second-harmonic beams are not plane-waves.

To find how the second-harmonic light propagates we will first write down the wave equation for the medium using SI units[2]. In the absence of charges and free currents in a non-magnetic medium, Maxwell's equations can be cast in the following form [3]

$$\nabla^2\vec{E}(\vec{r},t) + \frac{n^2}{c^2}\frac{\partial^2}{\partial t^2}\vec{E}(\vec{r},t) = -\mu_0\frac{\partial^2}{\partial t^2}\vec{P}(\vec{r},t) \tag{9}$$

[2] Most textbooks and literature on non-linear optics use Gaussian units.

[3] To arrive at this result, calculate $\nabla\times\nabla\times\vec{E}$, reverse the order of space and time derivatives and use the vector identity $\nabla\times\nabla\times\vec{E} = \nabla(\nabla\cdot\vec{E}) - \nabla^2\vec{E}$ with $\nabla\cdot\vec{E} = 0$.

In the two-step perturbative treatment of second-harmonic generation an electrical field $\vec{E_1}(\vec{r})\exp(i\omega t)$ generates a non-linear polarization profile $\vec{P_2}(r,\vec{t})$ that is inserted into the wave equation above. Using equation 2 for the non-linear polarization and considering only terms at the frequency 2ω of the second harmonic one finds [4]:

$$\nabla^2\vec{E_2}(\vec{r}) + \frac{(2\omega)^2}{c^2}\vec{E_2}(\vec{r}) = \frac{(2\omega)^2}{c^2}\vec{P_2}(\vec{r}) \tag{10}$$

If the radiation is dominantly in the forward direction one can use the so-called slowly-varying envelope approximation and rewrite the emitted field as

$$E_2(\vec{r}) \equiv A(\vec{r})exp(ik_2z) \tag{11}$$

This approximation is valid as long as $|\nabla A| \ll k_z|A|$. Within this approximation $\nabla^2\vec{A} = 0$, which greatly simplifies the wave equation and yields

$$\frac{\partial}{\partial z}\vec{A}(\vec{r}) = \frac{i\omega}{2nc}P_2(\vec{r})\exp(-ik_2z). \tag{12}$$

Note that equation 12 again expresses the importance of index or phase matching. The slowly-varying amplitude $A(\vec{r})$ exhibits a steady increase in the z-direction only when the right-hand side retains it's complex phase. This is the case when $P(\vec{r}) \propto \exp(ik_2z)$; i.e. when $n_\omega \approx n_{2\omega}$.

In order to study second harmonic generation for a realistic laser beam, we need to introduce the spatial profile $\vec{E_1}(\vec{r})$ of the incident beam. For a so-called Gaussian beam, propagating in the z-direction, the profile has the form

$$E_1(\vec{r}) = \frac{E_0}{1+i\tau}\exp\left(-\frac{x'^2+y'^2}{w_0^2(1+i\tau)}\right)\exp ik_1z. \tag{13}$$

This corresponds to a beam that has a Gaussian cross section at every point z along the propagation direction as depicted in Fig. 5. The minimal waist w_0 is reached at point $z = 0$. The parameter $\tau = 2z/b$ is the z-distance in units of the confocal parameter b. This confocal parameter is defined as

$$b \equiv w_0^2k_1 = w_0^2n_1\frac{2\pi}{\lambda_1}, \tag{14}$$

where $n_1 \equiv n(\omega)$ and $\lambda_1 \equiv 2\pi c/\omega$ both refer to the fundamental wave. Around the point $z = 0$ the beam is columnar; this columnar region of length b the beam has an almost constant width equal to w_0. The corresponding spatial profile of the nonlinear polarization at frequency 2ω is easily found via $P_2(\vec{r}) \propto E_1(\vec{r})^2$.

Let us first consider the “plane-wave” limit for a Guassian beam. This limit is reached when the incident laser beam is wide enough to (i) neglect focusing, and (ii) neglect transverse walk-off. The righthand side of Eq.12 is constant in this limit, making the integration over the crystal thickness extremely simple. If phase matching is satisfied ($\Delta k = 0$), the efficiency of the second-harmonic conversion is optimum and the intensity of the second harmonic $I_{2\omega}$ can be expressed in the simple form

[4] Note that the polarization $\vec{P}$ and the non-linear polarization $\vec{P}$ differ by a factor ε_0

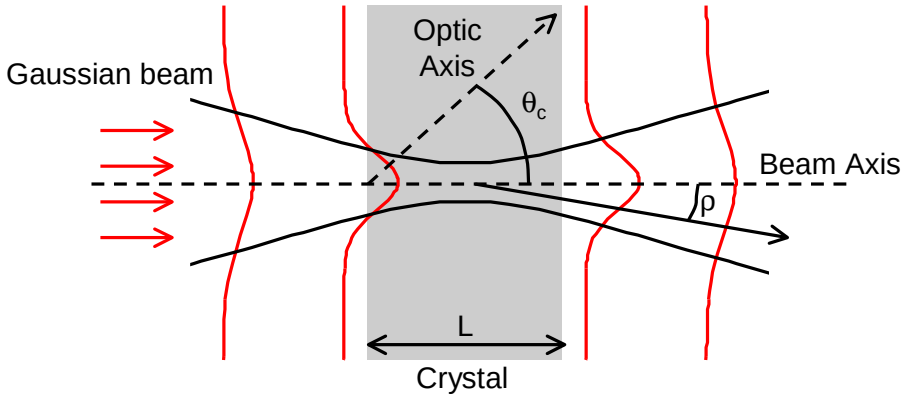

Figure 5: *Top view of typical focusing condition. An incident beam with a Gaussian profile is focused in the center of a nonlinear birefringent crystal, of which the c-axis is making an angle Θ_c (in the picture Θ_m) with the surface normal. The polarization direction of the incident light is vertical, or ordinary. The polarization direction of the generated second-harmonic light is horizontal, or extra-ordinary. Inside the crystal this light propagates at the so-called walk-off angle ρ with respect to the incident beam.*

$$I_{2\omega} = C^2 I_\omega^2 \frac{L^2}{\pi w_0^2}. \tag{15}$$

The field-gain coefficient C introduced here contains all material properties. For BBO in our geometry the field-gain coefficient measured by another group is $C \approx 1.71\times10^{-4}/\sqrt{W}$ [1], corresponding to a projected nonlinear coefficient $d_{eff} = 2.01$ pm/V.

2.6 Results for tightly focussed beams

When a laser beam is focussed strongly inside a non-linear crystal the “plane-wave” limit breaks down. The analysis of the efficiency of second-harmonic generation as given in references [3] and [4] does not result in a simple analytic expression. The numerical results are cast in form that resembles the expression for $I_{2\omega}$ given above

$$I_{2\omega} = C^2 I_\omega^2 \frac{Lb}{\pi w_0^2} h(B,\xi), \tag{16}$$

where they introduced the function $h(B,\xi)$ that is evaluated numerically. The function $h(B,\xi) = L/b$ in the plane wave limit, but will strongly deviate from this result in other regimes! To function introduces two new parameters ξ and B that are defined as

$$\xi \equiv \frac{L}{b}, \tag{17}$$

$$B \equiv \tfrac{1}{2}\rho\sqrt{(k_1 L)} = \frac{\rho L}{2w_0}\frac{1}{\sqrt{\xi}}. \tag{18}$$

The parameter ξ quantifies the effect of focusing; it compares the crystal thickness L with the confocal parameter b. The parameter B quantifies the effect of transverse beam walk-off. It compares the transverse walk-off distance ρL with the beam waist w_0, but also contains a factor $1/\sqrt{\xi}$.

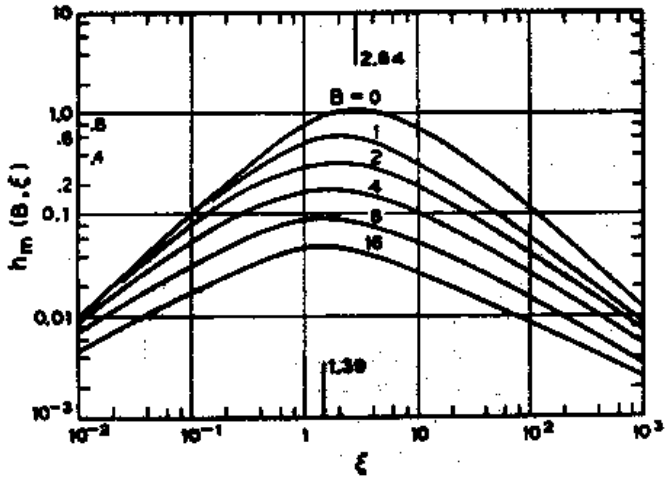

Figure 6: *Second-harmonic intensity, expressed in a scaled function $h(B,\xi)$, versus the focusing parameter $\xi = L/b$ for various walk-off conditions B (see text).*

The result of the numerical calculation of $h(B,\xi)$ is displayed in Figures 6 and 7, that are copied from Ref.[4]. From the curves in Fig. 6 we find that tighter focusing first leads to a linear increase in $h(B,\xi)$; the efficiency increases with $1/w_0^2$. Around $\xi = 1$, $h(B,\xi)$ experiences a maximum and for even tighter focussing the function $h(B,\xi)$ drops linearly as function of ξ; the efficiency of second harmonic generation decreases proportional to w_0^2. This general trend is observed for all values of the parameter B. The deteriorating effect of transverse beam walk-off on the conversion efficiency is clear from the differences between the curves in Fig. 6. The maximum possible value of $h(B,\xi)$ as a function of B is given by the solid line in Fig. 7. The general trend is clear; only if $B \ll 1$ the transverse beam walk-off is small enough to be neglected. If walk-off cannot be neglected it leads to a serious reduction of the maximum possible conversion efficiency.

Figures 6 and 6 contain results for optimum phase matching. In the plane-wave limit this condition corresponds to $\Delta k = 0$, and angle tuning is expected to lead to a symmetric $(\sin x)^2/x^2$ profile for $I_{2\omega}$ versus θ. Under tighter focusing conditions,

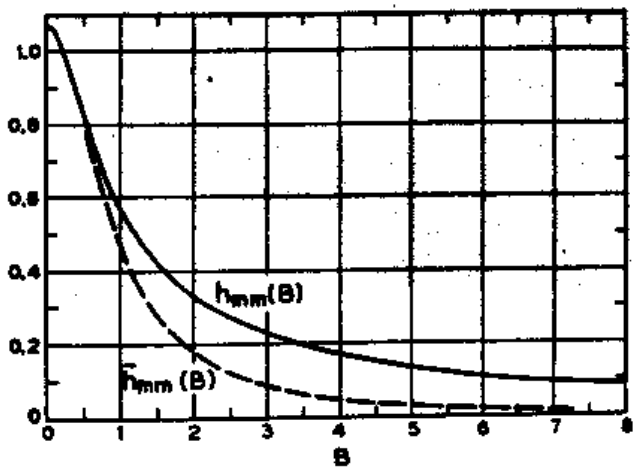

Figure 7: *Second-harmonic intensity, expressed in a scaled function $h(B, \xi)$, versus the walk-off parameter B. The solid curve corresponds to the process of second harmonic generation (see text).*

where many transverse wavevectors play a role, angle tuning is expected to become asymmetric, with a peak and extended wing on the positive Δk side. The explanation for this asymmetry is relatively simple: under strong focusing conditions the wave vectors in the incident beam are spread out over a cone, making the "average wavevector in the z-direction" smaller than for plane wave illumination. A tiny tilt of the crystal can compensate for this effect. Figure 8 shows the predicted angle dependence of the second harmonic intensity for the relatively tight focusing condition of $\xi = 5.0$ in the absence of beam walk-off $B = 0$ (this figure is a copy of Fig. 9 from ref. [4] that also contains similar curves for different values of ξ). Note the large asymmetry in combination with the oscillatory behavior, which is a remnant of the $(\sin x)^2/x^2$ dependence discussed above.

Even today the issue of phase matching in birefringent crystals is considered so complicated that well written articles on the subject still make it into respectable scientific journals [6]. So if you have some clever ideas when performing this experiment, don't hesitate to discuss them with your experimental assistant.

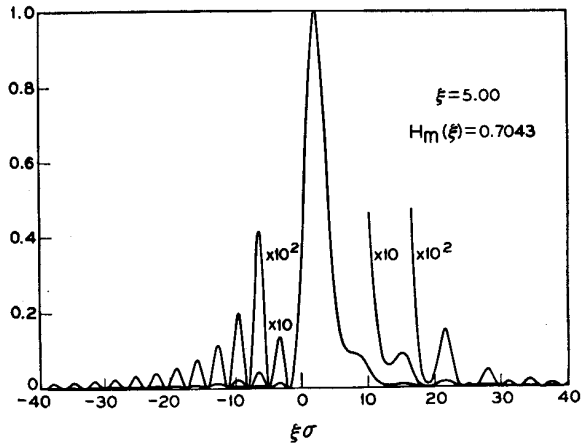

Figure 8: *Second-harmonic intensity as a function of the tilt angle of the birefringent crystal, expressed in terms of the phase mismatch* $\frac{1}{2}\Delta kL = \xi\sigma$ *for a relatively thick crystal* $\xi = 5.0$.

3 Experiment

Laser Safety in a nutshell

Before starting the experiment it is important that you read the manual and that you are aware of the risks of using a high power diode laser as is used in this experiment. It is of utmost importance that the **laser safety sign is switched on**, to warn possible visitors, and that you **always wear safety glasses** when the diode laser is on. You must realize that this diode laser can emit as much as 50 mW, which is about a factor 50x stronger than the typical HeNe laser used so far. Even a 4% reflection from the crystal is still 2 mW and strong enough to damage the human eye! What makes the radiation even more dangerous is it's wavelength in the near infrared, making it invisible to the naked eye.
To prevent any accidents it is also important to **shield the experimental setup and prevent possible reflection to leave the table**. When you are sitting behind the computer you certainly don't want to be surprised by a stray laser reflection that hits you in the eye! Use black metal shields or black cardboard for shielding.

Michiel .J.A. de Dood
Huygens Laboratorium 909a, tel. 071-527 5929

3.1 List of components for practicum: second harmonic generation

3.1.1 Diode laser components

Element Description	Quantity
Laser diode controller Thorlabs LDC202	1
Temperature controller Thorlabs TED200	1
50 mW laser diode type RLT9850MG	2

3.1.2 Optics

Element Description	Quantity
XYZ translation stage + holder collimating lens	1
Collimating lens (f=8mm NA=0.5) in tube mount	1
λ/2 plate @ 980 nm	1
Rotation stage / holder λ/2 plate	1
Lenses f=50 mm (AR coated at λ=1064nm)	2
Square-shaped lens holder for f=50mm lenses	2
Micro-metric translation stage for lens (range 15 mm)	1
Lens f=400mm (AR coated at λ=1064 nm)	1
Donut-shaped holder for f=400mm lens	1

3.1.3 Non-linear stage

Element Description	Quantity
Non-linear crystal in metal holder (nominal thickness 2 mm)	1
Non-linear crystal in black holder (nominal thickness 1 mm)	1
Motorized rotation stage with holder for nonlinear crystals	1
Controller motorized rotation stage	1

3.1.4 Detection stage

Element Description	Quantity
Photodiode (see documentation for specs)	1
Colored filter BG39 2 mm (see documentation for specs)	1
Oscilloscope (for monitoring and grounding)	1

3.1.5 Security devices

Element Description	Quantity
Security goggles	3
IR indicator card	1

3.2 Setting up the experiment

A sketch of the experimental setup was given as Fig. 1. Crucial aspects that determine the efficiency of the second-harmonic generation are: (i) the polarization direction of the incident light with respect to the crystalline axis, (ii) the angle between the incident beam and the crystal, (iii) the amount of focussing. All three aspects can and will be varied in the experiment.

A complete list of the available equipment necessary for this experiment is given in Section (4). Some finer details of this equipment will be given below.

First of all, we want to stress the importance of laser safety. NEVER switch the laser on without **safety goggles on**. Also don't allow stray reflections of laser light to exit your experimental setup, but block them physically. Also check that the warning lights outside the lab are operational.

Secondly, we note that **semiconductor diode lasers are easily damaged** and that you should strictly obey the switch on and switch off procedure (see below). As diode lasers function best under cooled and stable temperature conditions, you should first switch on the temperature controller (Thorlabs TED200) using the power button on the lower left. Use the buttons 'up' and 'down' to display the set temperature T_{SET}. Use the knob to set the temperature to roughly 15 °C and switch on the cooling by pressing the TEC on button (upper right). You can monitor the actual temperature by switching the display to T_{ACT}. When the cooling is working you can turn on the laser diode controller, which should start in the "current limit" mode with the display showing the set current limit. The LED labelled 'CG' should be on and the switches on the laser diode mount on the table should both be in the 'CG' position. (If this is not the case, ask for help). Use the 'up' and 'down' buttons to change the display to the laser current I_{LD}, put the driver in current mode ('MODE' is either constant current 'I' or constant power 'P') and check that the current is really zero (rotate the knob counterclockwise). Put on your safety goggles, (if you did not use them yet) and switch on the laser by pushing the laser on button (upper right). The display on the outside should now automatically light up and indicate that the laser is on. Slowly turn the knob to tune the laser current; the controller will beep whenever the maximum allowed laser current is reached. Switching off the device goes in the opposite order: first turn the current to zero, then push the button to switch off the laser and turn off the supply. If you are so careless to switch off the supply without first turning off the laser you are likely to destroy the diode laser, which is allergic to sudden current changes, and loose about 100 euros worth of equipment. Then switch of the cooling.

The infrared radiation, which is invisible and even dangerous to the naked eye, can be made visible by shining it onto special IR indicator cards. When illuminated by infrared light, these cards emit an orange-colored radiation (wear safety goggles all the time!). This conversion process, which seems impossible from an energetic point of view ($h\nu_{\mathrm{emission}} > h\nu_{\mathrm{absorption}}$) is made possible by the presence of long-living meta-stable states; these states are charged by TL light and thereby able to emit more energy than received when illuminated with infrared light.

You have two BBO crystals at your disposal, both cut at an angle of approximately 24.9°. The crystal in the black holder has a specified thickness of 1 mm, the crystal in the metal holder should be twice as thick. Either one of them can be mounted in the

crystal holder, which can be rotated very precisely, as it is connected to a combination of a stepper motor (step size 7.5°) and a 1/250 gearbox (see documentation for further specifications). This combination allows one to tune the angle between crystal and incident beam by steps of 0.03°. A small drawback of the described combination is the presence of hysteresis; you can only trust and reproduce the angle setting when you always come from same side. The stepping motor controller can be driven either manually or electronically from the computer. In both cases the angular scan is controlled by the same three knobs or controls: (i) direction (forward or backward), (ii) scan (enable or disable), and (iii) scan speed (internal clock or external "step-by-step"). First operate under manual control, but quickly switch to computer control for finer angle-tuning. Use the LabVIEW program "second-harmonic.vi".

On the detection side the light first passes a filter of BG39 colored glass, which is supposed to block the infrared light and pass the generated second-harmonic light. The documentation of this experiment should include curves of the wavelength-dependent optical transmission of BG39 per mm glass thickness. Note that the laser safety goggles also contain some type of color glass. The transmission characteristic of this glass (denoted as NY3) is also included in the documentation.

The photo detector that is used in this experiment is the standard type of physical practicum. It consists of a HUV4000 silicon photodiode with large area (40 mm^2 for easy alignment) and relatively low dark current, resulting in low dark current and therefore low current noise (current noise typically 10^{-14} A/$\sqrt{\mathrm{Hz}}$). Special care was taken to select low-noise electronics. As the intensity of the second-harmonic light is very small the detecting photodiode is typically operated at it's most sensitive setting (200 MΩ). This also makes it of vital importance to shield off any environmental light.

The focusing optics used in this experiment is relatively simple. There are in total four lenses available. The first lens is quite small and located at the end of the black tube close to the semiconductor laser. Positioning of this lens allows one to aim the laser beam and work either with a collimated beam, which is preferable, or with a focused beam, which also works but makes precise focusing on the BBO crystals quite difficult. This first lens has a focal distance of 8 mm and a numerical aperture as large as 0.5 (corresponding to a useful lens diameter of 8 mm). The other lenses that are available are two f=5 cm lenses and one f=40 cm lenses. These can be used to focus a collimated beam onto the BBO crystal and to re-image the light onto the detecting photodiode. Note that, in case of weak focusing the beam out of the BBO crystal might be small enough for the detecting photodiode, thus allowing us to leave the re-imaging lens out of the setup. Also note that the crucial parameter to describe the size of the focus is not the focal length of the lens, but rather the transverse size of the focal spot w_0, which depends just as much on the numerical aperature of the illuminating beam. As an alternative, but equivalent, measure one often uses the length of the focal spot, or the confocal parameter b (see Sec.2.1). In the experiment you are supposed to work both under tight focusing and weak focusing conditions. You should also move the focus through the crystal, i.e., perform "z tuning" by translating the focusing lens along the direction of the laser beam, to observe the consequences of focusing and defocusing on the efficiency of the second-harmonic generation.

3.3 Aiming for the first results

The first problem you encounter in this experiment is that you have to choose and set both the polarization direction of the laser light, as well as the orientation of the two crystals at convenient values. Having read the theoretical section and having looked at the rotation capabilities of the crystal mount, it shouldn't be too difficult to decide that the input polarization should be vertical and that the crystalline c-axis should be horizontal. Operate the laser diode at low output power and use the polarizer and $\lambda/2$ plate, in combination with the power meter, to find the required orientations with sufficient accuracy. **Wear safety goggles**. Hints: the polarization direction can be linked to the orientation of the optical table, by using the polarizer under both forward and backward illumination. Optimization for optical blocking is much more accurate than optimization for maximum throughput. Birefringent crystals don't perturb the optical polarization if this polarization is properly align with the crystalline c-axis, being either pure ordinary or pure extra-ordinary. Start with the thick crystal, which is expected to produce the strongest second-harmonic light.

When the incident polarization and crystalline axes are properly oriented, your next problem is proper focusing and angular tuning of the crystal. Simultaneous optimization of these two parameters is quite difficult. A first modest goal is to just get *some* second-harmonic light. For this you should adjust the focusing with the help of the IR indicator card and tune the crystalline angle manually. You can use a "business card" of white cardboard for "quick and dirty" optimization of P_2 or use the oscilloscope for accurate readout of the photodiode signal. In any case, wear safety goggles and operate the laser diode at large current; even at 50 mW laser power the expected second-harmonic power is only a few nW and barely visible.

When you have a measurable signal and optimized it for focusing you can shield the system, by enclosing it in a large cardboard box. More extended experiments, in particular any measurement of the second-harmonic intensity as a function of the crystal angle should be performed with a dedicated LabVIEW program. Documentation for this program should be available in the experimenting room.

At some point, better early than later on, you should also measure the laser intensity at the sample as a function of laser current. This measurement is easily performed with the photodiode on its least sensitive scale and shielded with a neutral density filter. Alternatively, the assistant can give you experimental results of earlier measurements of both the (current-dependent) laser power and the laser spot size.

3.4 Minimum experimental tasks (extensions are possible)

- Measure the angle dependence of second-harmonic intensity for at least 2 x 2 = 4 experimental situations (thin and thick crystal under both tight and mild focusing).
- Dependence of second-harmonic intensity as a function of the position of the BBO crystal within the focus of the laser beam (z-scan). Perform a z-scan of the lens for both the tight and mild focusing case.
- Discussion of the results and comparison with literature (among others ref.[4]).

Possible extensions could include:

- Detailed study of the asymmetry in the angular dependence of P_2 under strong focusing conditions.
- Using the thin crystal to compensate the walk-off effect for the thick crystal.
- Dependence of P_2 as function of numerical aperture by using a diaphragm.

References

[1] Y.R. Shen, *The principles of nonlinear optics* (John Wiley, New York, 1984).

[2] R.W. Boyd, *Nonlinear optics* (Academic Press, Boston, 1992).

[3] G.D. Boyd, A. Ashkin, J.M. Dziedzic and D.A. Kleinman, *Second-harmonic generation of light with double refraction*, Phys. Rev. **137**, A1305 (1965).

[4] G.D. Boyd and D.A. Kleinman, *Parametric interaction of focused Gaussian light beams*, J. of Appl. Phys. **39**, 3597 (1968).

[5] J.E. Bjorkholm, *Optical second-harmonic generation using a focused Gaussian laser beam*, Phys. Rev. **142**, 126-136 (1966).

[6] U.K. Sapaev, I.A. Kulagin, and T. Usmanov, *Theory of second-harmonic generation for limited laser beams in nonlinear crystals*, J. Opt. B: Quantum. Semiclass. Opt. **5** (2003) 355-356.

[7] D.N. Nikogosyan, *Handbook of nonlinear optical crystals* (Springer, Berlin,)